Nonlinear dynamic soil structure interaction in adjacent basement

Yetty Saragi[1*], Masyhur Irsyam[2], Roesyanto[3], Hendriyawan[2]

[1]Postgraduate Student of Departement Civil Engineering, University of North Sumatera (USU)
[2] Study Program of Civil Engineering, Institute of Technolgy Bandung (ITB)
[3] Departement Civil Engineering, University of North Sumatera (USU)

*yettyririssaragi@yahoo.com

Abstract. This research was conducted to analyze the lateral dynamic pressure distribution on the basement walls and amplification of earthquake motion on the surface using the finite element method Midas GTS-NX. Dynamic soil-structure interaction analysis was carried out by using a sensitivity program to influence soil conditions, earthquake acceleration in bedrock, basement depth, bedrock depth and stiffness of the basement structure with a distance between basements of 15,0 m. From this study, the lateral pressure distribution of the dynamic soil reaches the maximum at the base of the basement with an increase in pressure that is almost linear in soft and nonlinear soil conditions in medium and hard soil conditions. The greatest increase in gradient occurs at a depth of four per five basement walls measured from the surface to the bottom of the basement. The analysis shows that the dynamic lateral pressure distribution has a maximum value at the top end of the basement and tends to shrink to the bottom of the basement.

1. Introduction

High-level building structure in general can be divided into two main parts, namely the structure of the building which is above the ground surface and the structure of the building that is below the surface of the land. The structure of the building below the ground surface can be in the form of a basement called a basement. The function of the basement is to carry the weight of the upper structure into the soil and to resist lateral loads around the basement wall. One aspect of geotechnics that is often a problem in basement wall planning is the determination of lateral ground pressure in the basement wall due to earthquake which must be held by the basement wall. Therefore, it is necessary to analyze the interaction of the soil with the basement structure walls on the dynamic response. Research on interactions that occur between soil and structure has also been carried out, in order to obtain influence due to seismic loads (Sherif and Famg, 1984; Ishibasi and Fang, 1987; Wu and Finn, 1996; Hendriyawan and Meddi, 1996; Putu Sumiharta, 2002; I Nengah Sukertha, 2008; Imanuel Mangape, 2009). Further studies and analyzes are still needed to obtain more detailed dynamic response behavior of the soil-structure of the basement wall.

In this research, an analysis of the effect of local soil conditions on the interaction of soil dynamic responses to the basement wall structure is in the form of non-linear soil behavior in the form of a comparative study of the response of equivalent linear and nonlinear soil models to the basement wall structure which is also influenced by bedrock depth and acceleration surface earthquake waves.

2. Methodology

2.1. Soil structur interaction

Building construction based on its location to the ground surface can be divided into 2 (two) parts, namely the upper structure (upper structure) and the lower structure (sub structure). Both parts of this building have several differences in the method of analysis for design purposes. The difference is caused by differences in environmental conditions around the two parts of the construction building. For the upper structure, the state of the land does not directly influence the process of analysis and design. Meddi R. and Hendriyawan (1996) in their research results stated that for lower structures or embedded structures, the state of the soil plays an important role in the design of the external forces at work so that interactions between the soil and embedded structures need to be taken into account.

Interactions that occur can be in the form of the influence of earthquake loads on the dynamic response of the underground structure, or it can be the other way around, namely the influence of underground structures on the behavior of earthquake wave propagation from bedrock to surface. The type of material on the bedrock with characteristics of mass and stiffness will determine how much the earthquake load of the bedrock will change when the earthquake waves reach the surface. Analysis of lateral ground pressure in this study will use the help of the finite element program Midas GTS. Soil-structure interaction can be analyzed by 2 (two) methods, namely the direct method and the stepwise method (Kramer, Steven L., 1996). The system response is formulated as follows:

$$[M]\left\{\ddot{u}\right\} + [K^*]\{u\} = -[M]\left\{\ddot{u}_{ff}(t)\right\} \quad (1)$$

where $\left\{\ddot{u}_{ff}(t)\right\}$ is the acceleration of the free field at the nodal point boundary

Deformation in kinematic interactions can be calculated assuming that the foundation has rigidity but does not have mass. Kramer, 1996 states the equation of motion to represent this state, namely:

$$[M_{soil}]\left\{\ddot{u}_{KI}\right\} + [K^*]\left\{u_{KI}\right\} = -[M_{soil}]\left\{\ddot{u}_{b}(t)\right\} \quad (2)$$

Analysis of kinematic interactions results in the movement (relative to bedrock) of a foundation-structure system that has no mass due to kinematic interactions. This movement is combined with the movement of bedrock to obtain the total kinematic movement of the foundation-structure system and produce equation (3)

$$[M]\left\{\ddot{u}\right\} + [K^*]\{u\} = -[M]\left\{\ddot{u}_{b}(t)\right\} \quad (3)$$

Kartawijaya, Paulus (2007) mentioned that the soil-structure interaction causes an interaction force in the soil-structure interface that causes random waves and spreads to infinity, which is called radial damping. Soil materials provide attenuation called material attenuation.

The effect of soil-structure interaction on natural frequencies, damping ratios and displacement characteristics of the equivalent SDOF system can be shown in Figure 1 below. Figure 1 (a) shows that the natural frequency of an equivalent SDOF system is under a fixed-base system in addition to the stiffness ratio. The effect of soil-structure interaction on natural

frequency is slightly below the stiffness ratio, i.e when the soil stiffness is relatively large relative to the stiffness of the structure. For a fixed-base condition, the natural frequency of the equivalent system is the same as the natural frequency in the fixed-base condition.

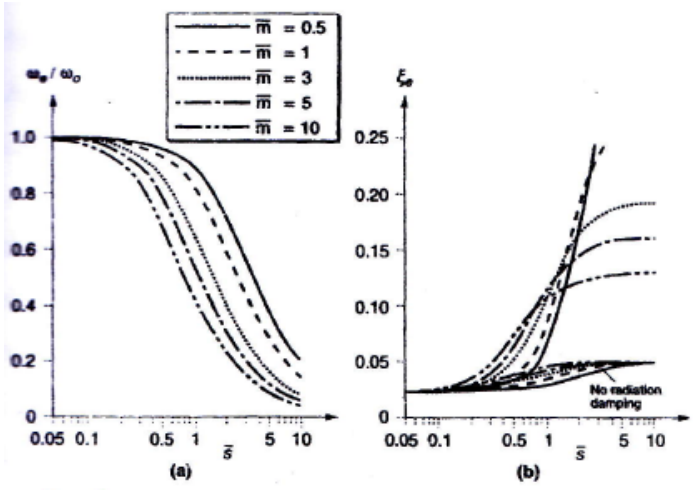

Figure 1. Effect of stiffness ratio and mass ratio on (a) natural frequency, (b) damping ratio of the soil-structure system ($\bar{h} = 1, \nu = 0.33, \xi = 0.025, \xi_g = 0.05$) (after Wolf, 1985)

Figure 1 (b) shows the effect of the soil-structure interaction on the damping ratio for the equivalent SDOF system. For fixed-base conditions, the damping ratio of the equivalent system is the same as the structural damping ratio, but as long as the stiffness ratio increases, the effect of soil attenuation will be more visible. At high stiffness ratios, structural damping is only a small part of the total damping in the system.

2.2 Dynamic Lateral Earth Pressure Analysis

This method is a modification method from the method that had been developed by Coulomb (1776). Mononobe and Okabe added additional vertical and horizontal forces due to the earthquake to the previous calculation. The basic equation of the Mononobe-Okabe method is the equilibrium of forces acting on a wedge (wedge) as below:

$$P_{AE} = \frac{1}{2}\gamma H^2 (1-k_v) K_{AE} \qquad (4)$$

with,

$$K_{AE} = \frac{\mathrm{Cos}^2(\phi-\theta-\beta)}{\mathrm{Cos}\,\theta\,\mathrm{Cos}^2\beta\,\mathrm{Cos}(\delta+\beta+\theta)\left\{1+\sqrt{\left[\frac{\mathrm{Sin}(\phi+\delta)\,\mathrm{Sin}(\phi-\theta-i)}{\mathrm{Cos}(\delta+\beta+\theta)\,\mathrm{Cos}(i-\beta)}\right]}\right\}^2}$$

and,

$$\beta = \tan^{-1}\left(\frac{k_h}{1-k_v}\right)$$

where ,

ϕ = shear angle in the ground
δ = sliding angle of the wall
i = inclination of land surface is behind the wall
β = back wall's slope to the vertical plane
W = weight of the collapse
P_{AE} = active pressure
R = resultant forces along the plane of collapse
k_hW = internal horizontal force due to weight alone
k_vW = vertical internal forces due to own weight
γ = soil density
K_{AE} = coefficient of active earth pressure with earthquake effects

Figure 2 shows the experimental results of Sherif and Fang (1984) in the form of dynamic active earth pressure distribution as a function of acceleration in a rigid wall that rotates at the top.It appears that at the bottom of the wall the value of the soil pressure is almost zero. While the peak is not zero and the amount increases according to the acceleration increase. The results of this experiment are in accordance with the predictions of Scott (1973), Matsuo and Ohara (1960) and Wood (1973).

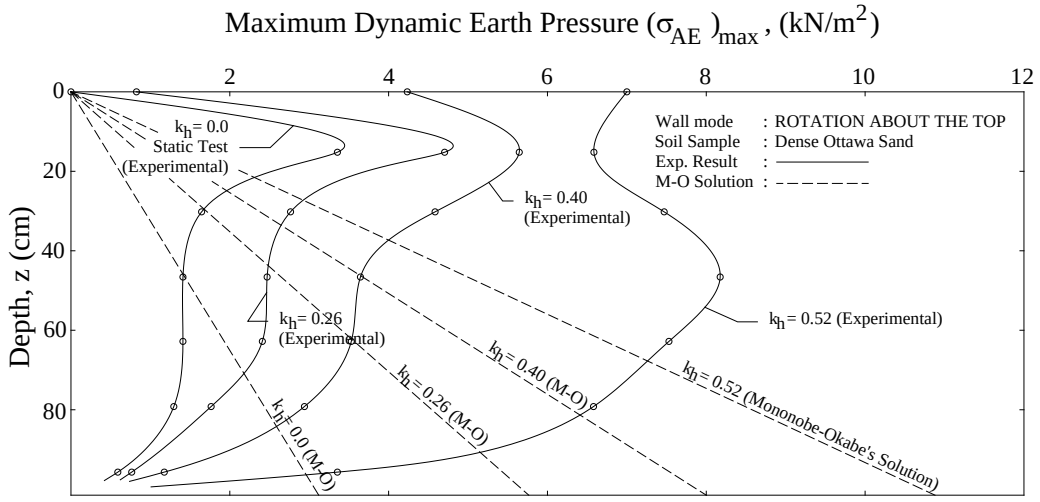

Figure 2 . Distribution of active active ground pressure rotating at the top as a function of horizontal acceleration (Sherif & Fang, 1984)

The results of these experiments can be concluded:

a. The dynamic active pressure distribution behind the rotating wall at the top is non-linear and the magnitude of this pressure reaches zero at the bottom of the wall. This active pressure increases at a distance of one third from the top of the wall.
b. The dynamic active pressure at the surface is not zero and the pressure at this surface increases with increasing acceleration.
c. The total dynamic active pressure capture point is 0.55H from the bottom of the wall and depends on the acceleration rate.

3. Result and discussion

The earthquake source zone used in this study is a subduction zone, which is a zone of earthquake events that occur near the boundary between the oceanic plates that pierce under the continental plate. The subduction zone referred to in this study is the megathrust zone, which is a sub-earthquake subduction from the surface to a depth of 50 km. The classification of local soil is one of the important stages, because different soil classifications will provide different soil responses in propagating waves. The most commonly used classification is based on shear wave data obtained from direct measurements or other field test correlation results (eg SPT). Soil classification based on soil profile to a depth of 30m.

Local soil data used in this study is data from 407 SPT points in Jakarta. In this study the silt layer is modeled as a clay layer, so that the type of soil consists only of sand and clay.

At this stage, an analysis of soil structure interaction was carried out to determine the amplification factor of the surface response due to the basement compared to the free field conditions using the Midas GTS NX. Analysis is done by calculating earthquake characteristic parameters based on the failure mechanism, soil conditions based on the shear wave propagation velocity, frequency content of input motion, earthquake acceleration in bedrock, basement depth and distance of the closest building to the basement. Land is modeled as solid elements and building structures are modeled as beam and column elements, left and right boundaries are modeled with the closest building distance to the basement. Earthquake load which is synthetic earthquake data is given at the bottom layer (baserock).

The experiment with basement distance 15,0 m and different basement depth 13,0 m and 10,0 m, the result can be seen in Figure 3 and Table 1-2.

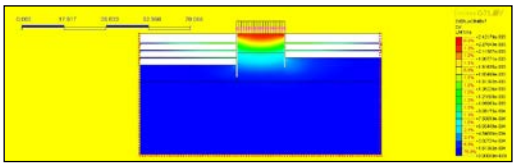

MODE 1: f(1.30987), DX(V)

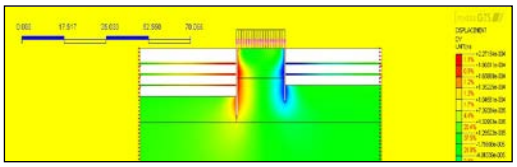

MODE 1: f(1.30987), DY(V)

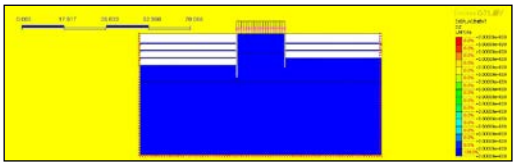

MODE 1: f(1.30987), DZ(V)

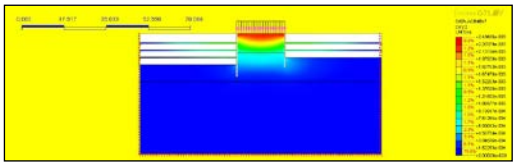

MODE 1: f(1.30987), DXYZ(V)

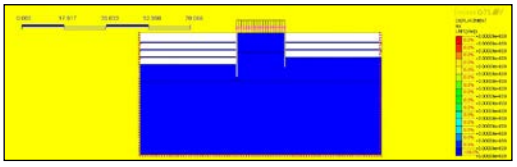

MODE 1: f(1.30987), RX(V)

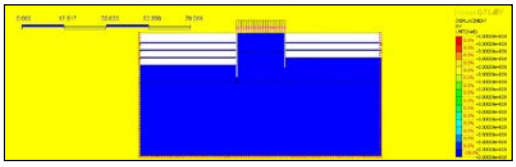

MODE 1: f(1.30987), RY(V)

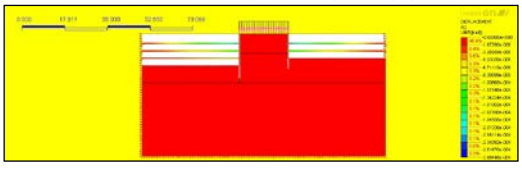

MODE 1: f(1.30987), RZ(V)

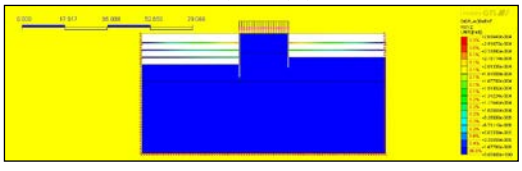

MODE 1: f(1.30987), RXYZ(V)

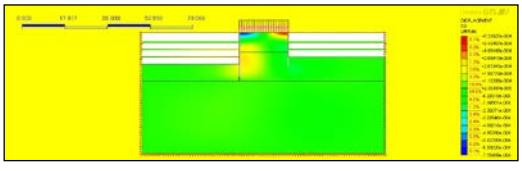

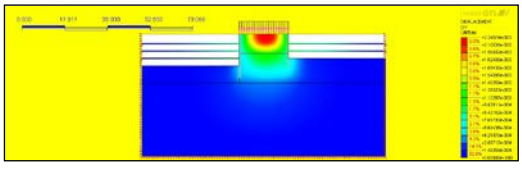

MODE 2: f(1.84269), DX(V)

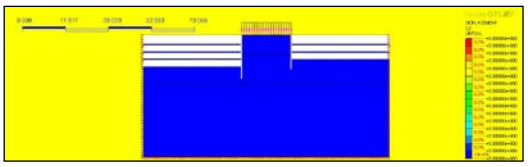

MODE 2: f(1.84269), DY(V)

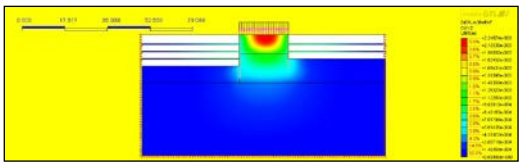

MODE 2: f(1.84269), DZ(V)

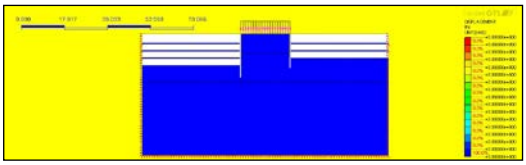

MODE 2: f(1.84269), DXYZ(V)

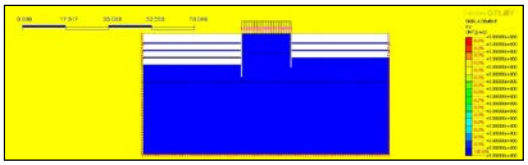

MODE 2: f(1.84269), RX(V)

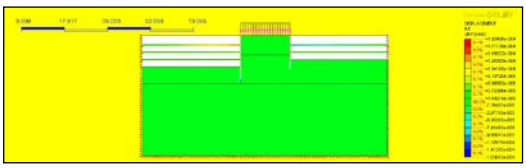

MODE 2: f(1.84269), RY(V)

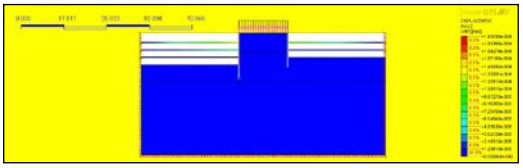

MODE 2: f(1.84269), RZ(V)

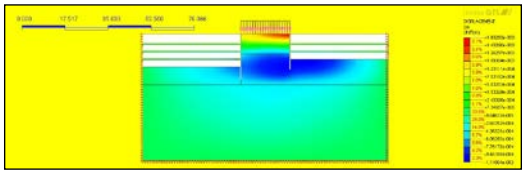

MODE 2: f(1.84269), RXYZ(V)

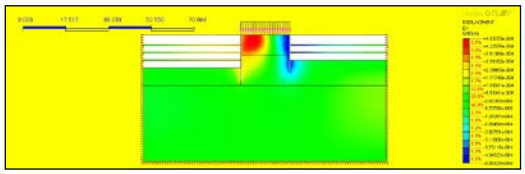

MODE 3: f(1.98886), DX(V)

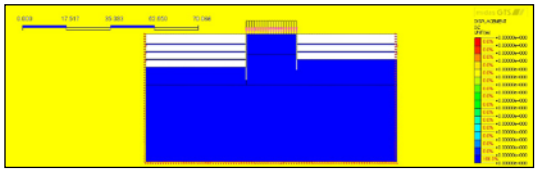

MODE 3: f(1.98886), DY(V)

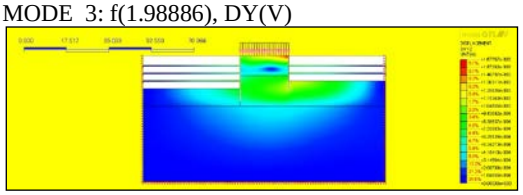

MODE 3: f(1.98886), DZ(V)

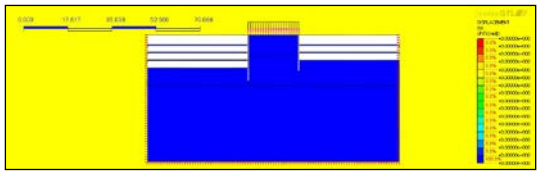

MODE 3: f(1.98886), DXYZ(V)

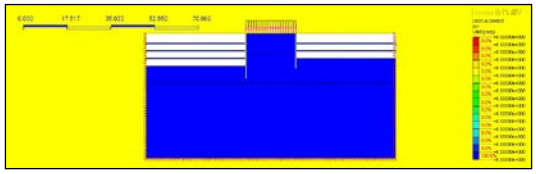

MODE 3: f(1.98886), RX(V)

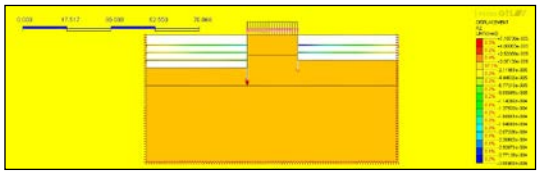

MODE 3: f(1.98886), RY(V)

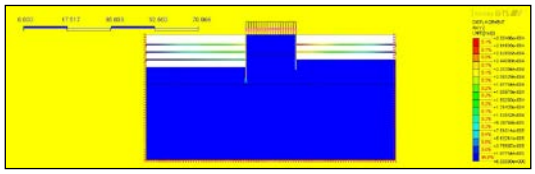

MODE 3: f(1.98886), RZ(V)

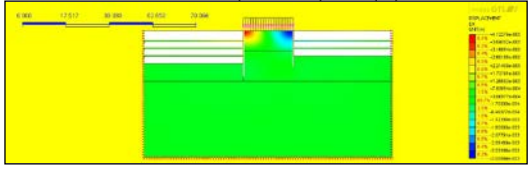

MODE 3: f(1.98886), RXYZ(V)

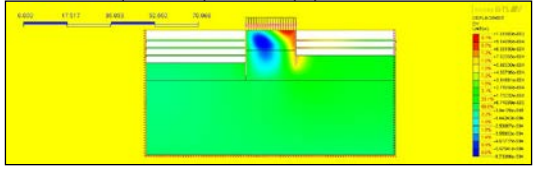

MODE 4: f(2.33433), DX(V)

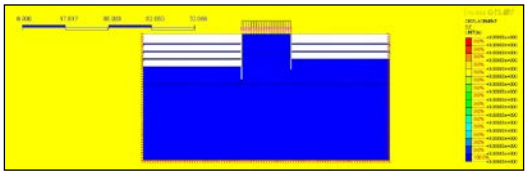

MODE 4: f(2.33433), DY(V)

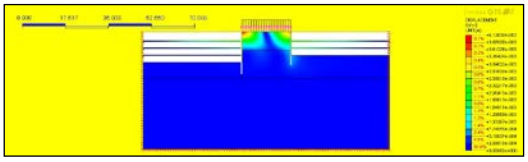

MODE 4: f(2.33433), DZ(V)

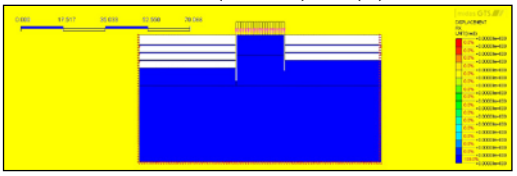

MODE 4: f(2.33433)

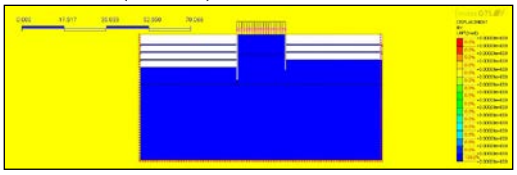

MODE 4: f(2.33433), RX(V)

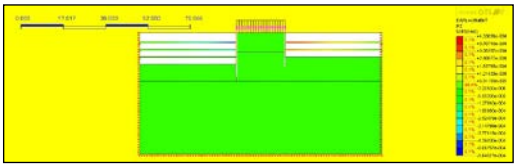

MODE 4: f(2.33433), RY(V)

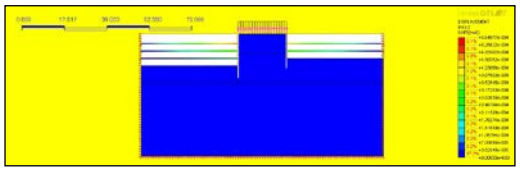

MODE 4: f(2.33433), RZ(V)

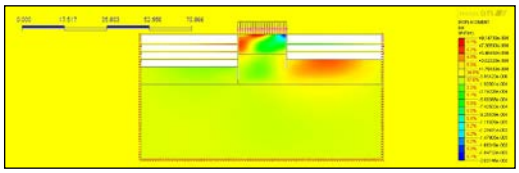

MODE 4: f(2.33433), RXYZ(V)

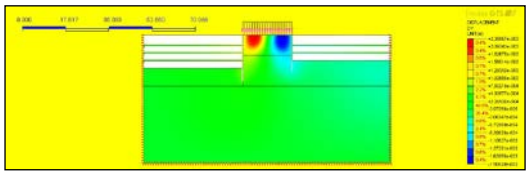

MODE 5: f(2.43624), DX(V)

MODE 5: f(2.43624), DY(V)

MODE 5: f(2.43624), DZ(V)

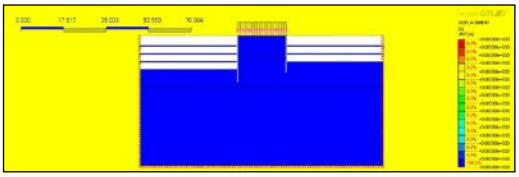

MODE 5: f(2.43624), DXYZ(V)

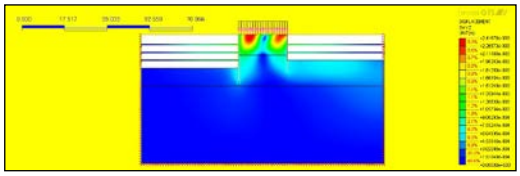

MODE 5: f(2.43624), RX(V)

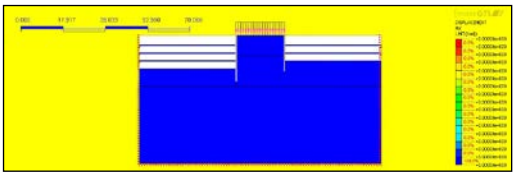

MODE 5: f(2.43624), RY(V)

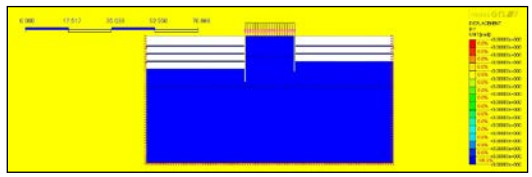

MODE 5: f(2.43624), RZ(V)

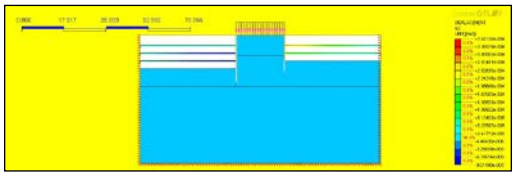

MODE 5: f(2.43624), RXYZ(V)

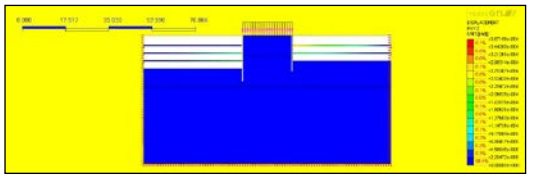

RESPONSE SPEC 1(1), FX(V)

RESPONSE SPEC 1(1), FY(V)

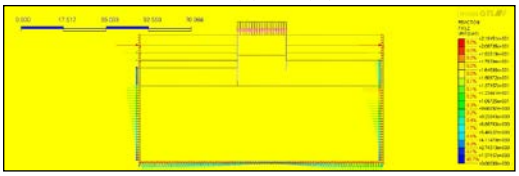

RESPONSE SPEC 1(1), FZ(V)

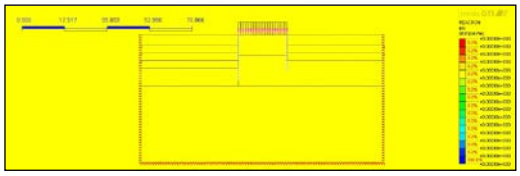

RESPONSE SPEC 1(1), FXYZ(V)

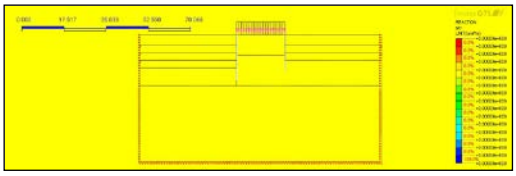

RESPONSE SPEC 1(1), MX(V)

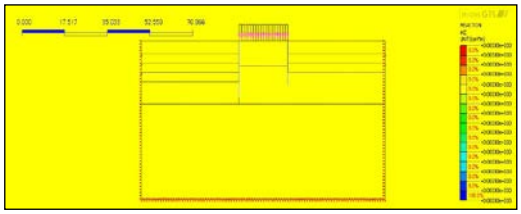

RESPONSE SPEC 1(1), MY(V)

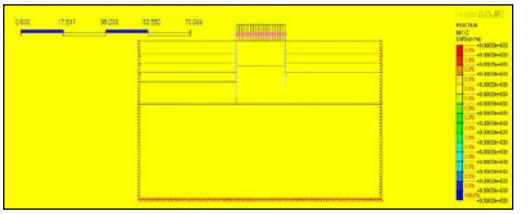

RESPONSE SPEC 1(1), MZ(V)

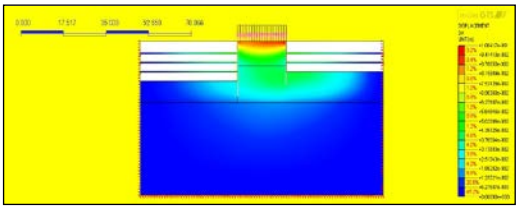

RESPONSE SPEC 1(1), MXYZ(V)

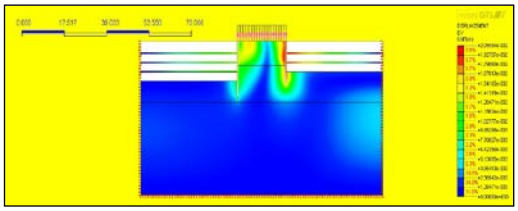

RESPONSE SPEC 1(1), DX(V)

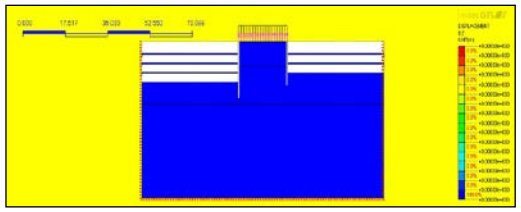

RESPONSE SPEC 1(1), DY(V)

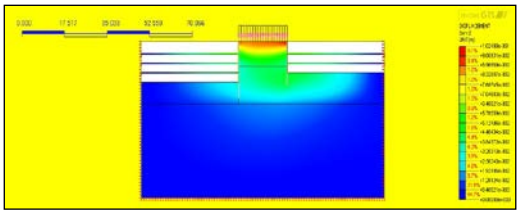

RESPONSE SPEC 1(1), DZ(V)

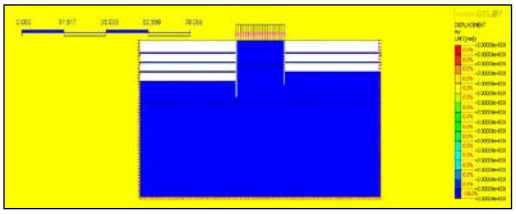

RESPONSE SPEC 1(1), DXYZ(V)

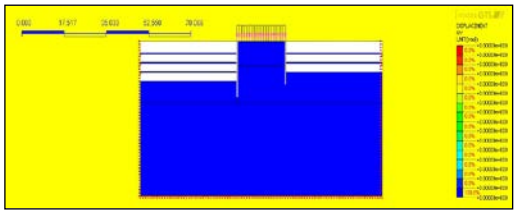

RESPONSE SPEC 1(1), RX(V)

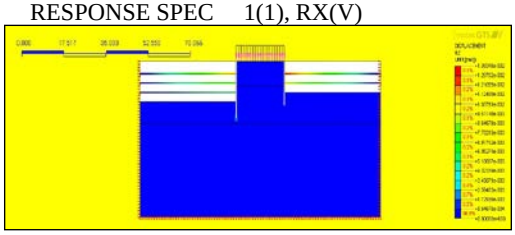

RESPONSE SPEC 1(1), RY(V)

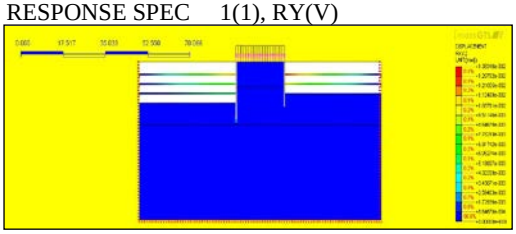

RESPONSE SPEC 1(1), RZ(V)

RESPONSE SPEC 1(1), RXYZ(V)

Figure 3. Nonlinear dynamic responce

Table `1. Maximum value in Mode of nonlinear dynamic responce

Information	Dx	Dy (m)	Dz (m)	Dxyz (m)	Rx (m)	Ry (rad)	Rz (rad)	Rxyz (rad)	(rad)
Mode 1		$2.4\ 10^{-3}$	$2{,}3\ 10^{-4}$	0	$2.4\ 10^{-3}$	0	0	0	0
Mode 2		$6{,}3\ 10^{-4}$	$2{,}3\ 10^{-3}$	0	2,2 10-3	0	0	$-7{,}4\ 10^{-5}$	0
Mode 3		$1{,}6\ 10^{-3}$	$4{,}6\ 10^{-4}$	0	$1{,}7\ 10^{-3}$	0	0	$-2{,}1\ 10^{-5}$	0
Mode 4		$4{,}1\ 10^{-3}$	$1{,}0\ 10^{-3}$	0	$4{,}1\ 10^{-3}$	0	0	$-3{,}2\ 10^{-5}$	0
Mode 5		$9{,}1\ 10^{-4}$	$2{,}4\ 10^{-3}$	0	$2{,}4\ 10^{-3}$	0	0	$5{,}3\ 10^{-5}$	$2{,}3\ 10^{-5}$

Table 2. Maximum value Force-Momen-SSI

Information			Maximum Value
Force	Fx	(tonf)	$2{,}2\ 10^{-1}$
	Fy	(tonf)	3,9
	Fz	(tonf)	0
	Fxyz	(tonf)	2,2 10
Momen	Mx	(tonf∗m)	0
	My	(tonf∗m)	0
	Mz	(tonf∗m)	0
	Mxyz	(tonf∗m)	0
SSI	Dx	(m)	$1{,}0\ 10^{-1}$
	Dy	(m)	$2{,}1\ 10^{-2}$
	Dz	(m)	0
	Dxyz	(m)	$1{,}0\ 10^{-1}$
	Rx	(m)	0
	Ry	(m)	0
	Rz	(m)	0
	Rxyz	(m)	0

4. Conclusion

It appears that at the bottom of the wall the value of the soil pressure is almost zero. While the peak is not zero and the amount increases according to the acceleration increase. The difeerent basement depth gives different results for each basement wall being reviewed. Soil structure Interaction (SSI) in adjacent basement give displacent 0,10 m.

Reference

[1]. ASCE/SEI-7-10, American Society of Civil Engineers, Minimum Design Loads for Buildings and Other Structures.

[2]. Arfiadi, Y., et.al. (2013). "Perbandingan Spektra Desain Beberapa Kota Besar di Indonesia Dalam SNI Gempa 2012 dan SNI Gempa 2002". *Konferensi Nasional Teknik Sipil 7 (KoNTekS 7), Universitas Sebelas Maret, Surakarta.*

[3]. Asrurifak, M. (2007). *Metode Penggunaan Hazard Software USGS Software for Probabilistic Seismic Hazard Analysis (PSHA).* Thesis Magister. Institut Teknologi Bandung.

[4]. Asrurifak, M., et.al. (2010). "Development of Spectral Hazard Map for Indonesia with a Return Period of 2500 Years Using Probabilistic Method". *Civil Engineering Dimension, Vol 12, Issue 1,52-62.*

[5]. Asrurifak, M., et.al. (2010)."Development of Spectral Hazard Map for Indonesia with a Return Period of 2500 Years Using Probabilistic Method". *Civil Engineering Dimension, Vol. 112, issue 1, 52-62*

[6]. Asrurifak, M., et.al. (2012)."Peta Deagregasi Hazard Gempa Indonesia Untuk Periode Ulang Gempa 2475 Tahun". *Pertemuan Ilmiah Tahunan XVI, PIT-HATTI, Jakarta.*

[7]. Assimaki, D.,et.al (2000). "Model for Dynamic Shear Modulus and Damping for Granular Soils". *Journal of Geotechnical and Geoenvironmental Engineering* ,126(10). 859-869

[8]. Atkinson, J.H., Bransby, P.L. (1978). *The Mechanics of Soils, An Introduction to Critical State Soil Mechanics.* McGraw-Hill Book Company (UK) Limited.

[9]. Awando, B. (2011). *Building Replacement Cost for Seismic Risk Assessment in Palbapang Village Bantul Yogyakarta Indonesia.* Thesis Magister. Gadjah Mada University dan University of Twente.

[10]. Azlan,A. et,al. (2006). "Development at Synthetic Time Histories at Bedrock for Kuala Lumpur". *Proceeding APSEC 2006, Kuala Lumpur, Malaysia*